PHƯƠNG PHÁP ĐIỀU KHIỂN CHUYỂN ĐỔI MẶT PHẲNG PHA DÙNG CHO CÁC HỆ THỐNG CÓ ĐỘ GIẢM CHẤN THẤP
PHASE PLANE SWITCHING CONTROL METHOD FOR LOW DAPING SYSTEM

Tu Diep Cong Thanh

Mechatronics Department, HCMC University of Technology, Viet Nam

BẢN TÓM TẮT

Một loại cơ cấu tác động phỏng sinh học dùng khí nén được ứng dụng rộng rãi vì những ưu điểm như: tính rắn chắc, tỉ số công suất/ khối lượng lớn, dễ bảo trì và tính an toàn cố hữu,v.v.. và được quan tâm trong những thập niên gần đây như một loại cơ cấu thay thế lý thú cho thủy lực và động cơ điện. Tuy nhiên, vẫn tồn tại một số khuyết điểm như khí bị nén và độ giảm chấn thấp đã tạo ra những chuyển động bị dao động. Vì vậy, nó không dễ giám sát đáp ứng của hệ thống trong điều kiện thay đổi quán tính tải với tốc độ cao.

Để giám sát và có đáp ứng của hệ thống tốt, một loại thiết bị có hệ số giảm chấn thay đổi dùng chất lỏng từ tính được gắn trực tiếp vào các khớp của tay máy. Sự hòa lẫn của bộ điều khiển PID truyền thống và phương pháp điều khiển chuyển đổi mặt phẳng pha sẽ mang lại một bộ điều khiển mới lạ. Kết quả thực nghiệm sẽ minh chứng cho những ảnh hưởng của giải thuật được đề xuất trong điều kiện quán tính tải bên ngòai thay đổi.

ABSTRACT

A novel pneumatic artificial muscle actuator (PAM actuator), which has achieved increased popularity to provide the advantages such as high strength and high power/weight ratio, low cost, compactness, ease of maintenance, cleanliness, readily available and cheap power source, inherent safety and mobility assistance to humans performing tasks, has been regarded during the recent decades as an interesting alternative to hydraulic and electric actuators. However, some limitations still exist, such as the air compressibility and the lack of damping ability of the actuator bring the dynamic delay of the pressure response and cause the oscillatory motion. Then it is not easy to realize the performance of transient response of pneumatic artificial muscle manipulator (PAM manipulator) due to the changes in the external inertia load with high speed.

In order to realize satisfactory control performance, a variable damper – Magneto-Rheological Brake (MRB), is equipped to the joint of the manipulator. Superb mixture of conventional PID controller and a phase plane switching control (PPSC) method brings us a novel controller. This proposed controller is appropriate for a kind of plants with nonlinearity, uncertainties and disturbances. The experiments were carried out in practical PAM manipulator and the effectiveness of the proposed control algorithm was demonstrated through experiments, which had proved that the stability of the manipulator can be improved greatly in a high gain control by using MRB with PPSC method and without regard for the changes of external inertia loads.

1. INTRODUCTION

Industrial robots have used three primary power sources: electric motors, hydraulic cylinders and pneumatic cylinders. Each of these actuation systems has advantages and disadvantages (Table 1). For most robotic applications, the common actuator technology is electric system with very limited use of hydraulics or pneumatics. But electrical systems suffer from relatively low power/weight ratio and especially in the case of human friendly robot, or human coexisting and collaborative systems such as a medical and welfare fields.

These advantages above have led to the development of novel actuators such as the

McKibben Muscle, Rubber Actuator and PAM manipulators. The PAM manipulator has been applied to construct a human-friendly therapy robot. For example, 2-dof robot for functional recovery therapy driven by pneumatic muscle was developed [1], artificial muscle actuators for biorobotic systems [2], and a pneumatic muscle hand therapy device [3]. However, the air compressibility and the lack of damping ability of the pneumatic muscle actuator bring the dynamic delay of the pressure response and cause the oscillatory motion. Therefore, it is not easy to realize the performance of transient response with high speed and with respect to various external inertia loads in order to realize a human-friendly therapy robot.

The limitations of the PAM manipulators have promoted research into a number of control strategies, such as a Kohonen-type neural network for the position control of robot end-effector within 1 cm after learning [4]. Recently, the authors have developed a feed forward neural network controller and accurate trajectory following was obtained, with an error of 1[^{o}] [5]. After applying a feed forward + PID-type controller approach, the authors are turning to an adaptive controller [6]. Recently, the authors have announced that the position regulation of the joints of their arm prototype is better than ±0.5[^{o}] [7]. In addition, sliding mode control [8], fuzzy PD+I learning control [9], robust control [10], and so on, have been applied to control the PAM manipulator. Though these systems were successful in addressing smooth actuator motion in response to step inputs, the manipulator must be controlled slowly in order to get stable, accurate position control and the external inertia load was also assumed to be constant or slowly varying. Therefore, it is necessary to propose a new control algorithm, which is applicable to a very compressible pneumatic muscle system with various loads.

Many new control algorithms based on a neural network have been proposed. An intelligent control using a neuro-fuzzy network was proposed [11]. An adaptive controller based on the neural network was applied to the artificial hand [12]. Here, the neural network was used as a controller, which had the form of compensator or inverse of the model. It was not easy to apply these control algorithms to the quickly-changing inertia load systems and to reconcile both damping and response speed in high gain control.

To over come these problems, a new technology, Electro-Rheological Fluid Damper (ER Damper), has been applied to the PAM manipulator [13. However, some limitations still exist, such as ER Fluid (ERF) requires extremely high control voltage (kV) which is problematical and potentially dangerous, only operates in a narrow range of temperature which can not be applied for PAM manipulator, and has also the characteristics of nonlinearity. Because ERF has many unacceptable disadvantages, Magneto-Rheological Fluid (MRF) attracts people's attention with these advantages in Table 2, in recent years. MR fluid is similar to ER fluid but is 20~50 times stronger in the yield stress. It can also be operated directly from low-voltage power supplies and is far less sensitive to contaminants and temperature.

Thus, the goal of this paper is to implement a magneto-rheological brake, to develop a fast, accurate pneumatic control system and without regard for the changes of external inertia loads. Superb mixture of conventional PID controller and a PPSC method bring us a novel controller. This proposed controller is appropriate for a kind of plants with nonlinearity uncertainties and disturbances. The experiments were carried out in practical PAM manipulator and the effectiveness of the proposed control algorithm was demonstrated through experiments, which had proved that the stability of the manipulator can be well improved in a high gain control by using MRB with PPSC method and without decreasing the response speed and low stiffness of manipulator.

2. EXPERIMENTAL SETUP

2.1 Experimental apparatus

The schematic diagram of the pneumatic artificial muscle manipulator is shown in Fig. 1. The hardware includes an IBM compatible personal computer (Pentium 1 GHz), which calculates the control input, controls the proportional valve (FESTO, MPYE-5-1/8HF-710 B) and Magneto-Rheological Rotary Brake (LORD, MRB-2107-3 Rotary Brake), through D/A board (Advantech, PCI 1720), and two pneumatic artificial muscles (FESTO, MAS-10-N-220-AA-MCFK). The braking torque of

magneto-rheological rotary brake is controlled by D/A broad through voltage to current converter, Wonder Box Device Controller Kit (LORD, RD-3002-03). And the lists of experimental hardware are tabulated in Table 3. The structure of the artificial muscle is shown in Fig. 2. The rotating torque is generated by the pressure difference between the antagonistic artificial muscles and the external load is rotated as a result (Fig. 4). A joint angle, θ, is detected by rotary encoder (METRONIX, H40-8-3600ZO) and the air pressure into each chamber is also measured by the pressure sensors (FESTO, SDE-10-10) and fed back to the computer through 24-bit digital counter board (Advantech, PCL 833) and A/D board (Advantech, PCI 1711), respectively. The external inertia load could be changed from 20 [kg·cm^2] to 200 [kg·cm^2], which is a 1,000 [%] change with respect to the minimum inertia load condition. The experiments are conducted under the pressure of 0.4 [MPa] and all control software is coded in C program language. A photograph of the experimental apparatus is shown in Fig. 3.

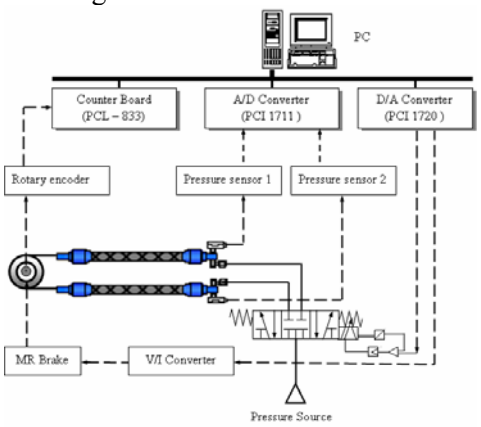

Fig. 1 Schematic diagram of PAM manipulator

2.2 Characteristics of the PAM manipulator

The PAM is a tube clothed with a sleeve made of twisted fiber-code, and fixed at both ends by fixtures. The muscle is expanded to the radial direction and constricted to the vertical direction by raising an inner pressure of the muscle through a power-conversion mechanism of the fiber-codes. The PAM has a property like a spring, and can change its own compliance by the inner pressure. A few slide parts and a little friction are favorable to a delicate power control. But the PAM has characteristics of hysteresis, non-linearity and low damping. Particularly, the system dynamics of the PAM changes drastically by the compressibility of air in cases of changing external loads. In our experiments, the external load changed about 1,000 [%] with respect to the minimum inertia condition.

Fig. 2 Structure of the PAM

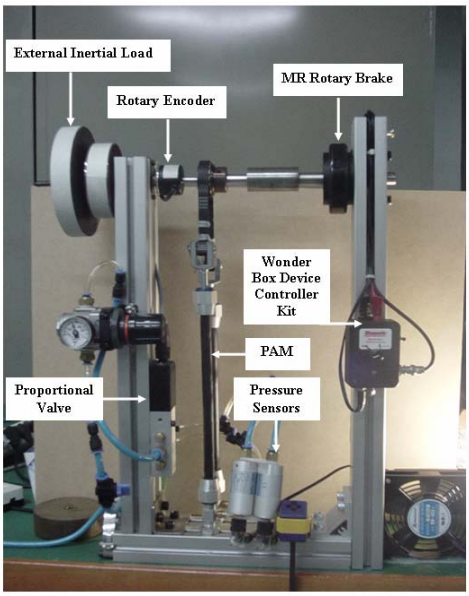

Fig. 3 Photograph of the experimental apparatus

When using the PAM for the control of manipulator, it is necessary to understand its characteristics such as the hysteresis, nonlinearity and so on. Therefore the following experiments are performed to investigate the characteristics of the PAM. Figures 5 and 6 demonstrate the hysteresis characteristics for the joint. This hysteresis can be shown by rotating a joint along a pressure trajectory from $P_1=P_{max}$, $P_2=0$ to $P_1=0$, $P_2=P_{max}$ and back again by incrementing and decrementing the pressures by controlling the proportional valve. The hysteresis of the PAM is shown in Fig. 6. The width of the gap between the two curves depends on how fast the pressures are changed; the slower the change in the pressures, the narrower the gap. The trajectory, control input to the proportional valve, velocity, and pressure of each chamber of the PAM are depicted in Fig. 5. The velocity is numerically computed from

the position. Near the extreme values, the joint velocity decreases since the increase in exerted force for a constant change in pressure is less.

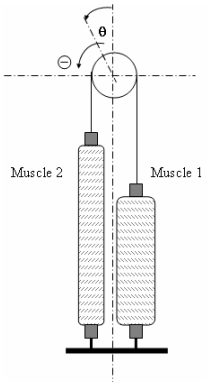

Fig. 4 Working principle of PAM manipulator

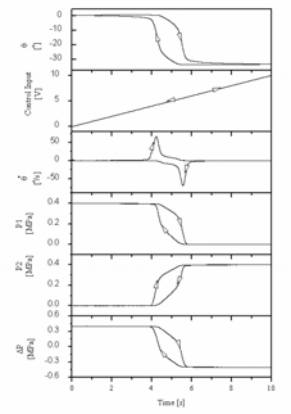

Fig. 5 Characteristics PAM manipulator

2.3 Characteristics of MRB

Construction of MR rotary brake was shown in Fig. 7. The rotor in Fig. 7 is fixed to the shaft, which can rotate in relation to housing. Between rotor and housing there is a gap filled with MR fluid. Braking torque of magneto-rheological rotary brake can be controlled by the electric current in its coil. An apparent viscosity of MR fluid is changed at few milliseconds after the application of a magnetic field, and goes back to the normal viscosity with no magnetic field.

The following experiments are performed to investigate the characteristics of MRB, which measurement data is shown in Fig. 8 and Table 4. MRB is connected with a torque transducer and a servomotor in series. In this experiments, the rotational speed is changed from 100 [rpm] to 1000 [rpm] and the current applied for MRB is changed from 0 [A] to 1[A]. The reason for choosing this range of rotational speed and current is that the response of system does not reach to 1000 [rpm] and the maximum current applied for MRB is 1 [A]. Figure 8 shows the damping torque with respect to the change of the input current (a) and rotational speed (b) of MR Brake. From Fig. 8, it is clear that the damping torque of MRB is independent of rotational speed and almost proportional to input current. Thus an equation (1) holds between the inputs current I and damping torque T_b

$$T_b = f(I) = a + bI \tag{1}$$

Here, a and b are constant.

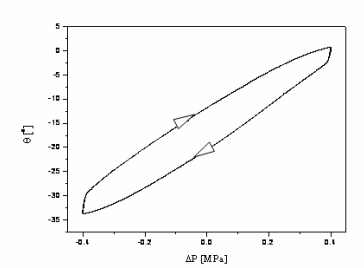

Fig. 6 Hysteresis of PAM manipulator

3. PHASE PLANE SWITCHING CONTROL ALGORITHM

3.1 The overall control system

The strategy of PID control has been one of the sophisticated methods and the most frequently used control algorithms in the industry. This is because that the PID controller has a simple form and strong robustness in broad operating area. To control this PAM manipulator, a conventional PID control algorithm was applied in this paper as the basic controller. The controller output can be expressed in the time domain as:

$$u(t) = K_p e(t) + \frac{K_p}{T_i}\int_0^t e(t)dt + K_p T_d \frac{de(t)}{dt} \tag{2}$$

Taking the Laplace transform of (2) yields:

$$U(s) = K_p E(s) + \frac{K_p}{T_i s} E(s) + K_p T_d E(s) \tag{3}$$

and the resulting PID controller transfer function of:

$$\frac{U(s)}{E(s)} = K_p\left(1 + \frac{1}{T_i s} + T_d s\right) \tag{4}$$

A typical real-time implementation at sampling sequence k can be expressed as:

$$u(k) = K_p e(k) + u(k-1) + \frac{K_p T}{T_i} e(k) + K_p T_d \frac{e(k) - e(k-1)}{T} \tag{5}$$

where $K_p, T_i, T_d, u(k)$, and $e(k)$ are the proportional gain, integral time, derivative time, control input to the control valve and the error between the desired set point and the output of joint, respectively. In addition, MRB is one of effective methods to improve the control performance of the PAM manipulator by reconciling both the damping and response speed because it works in only the regions

where the acceleration or deceleration is too high. The structure of the proposed PPSC method is shown in Fig. 9. Here, s is Laplace operator, T_a is torque produced by manipulator, T_c is constant torque and K_{ED} determines a gain for the torque proportional to the angular speed $\dot{\theta}$, V_c is a control voltage of source calculated from Eq. (1) to produce T_c. A direction of a damping torque is every time opposite to the rotary direction of the arm. So Eq. (6) below indicates that the damper produces a torque T_b.

$$T_b = \left(K_{ED}\dot{\theta} + T_c\right) sign(\dot{\theta}) \quad (6)$$

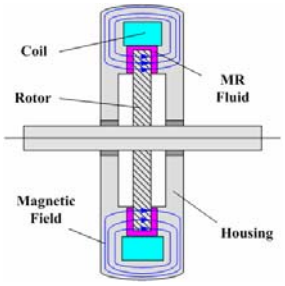

Fig. 7 Construction of MRB

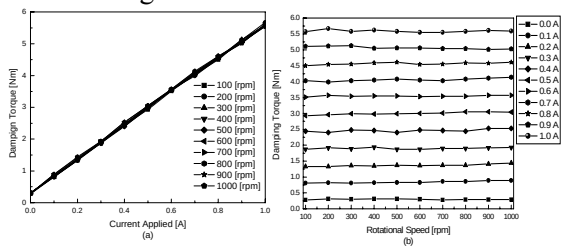

Fig. 8 Characteristics of MRB

3.2 Phase plane switching control method

The damping torque T_b improves the damping performance of the manipulator. Since the damping torque every time acts in the direction against the rotational direction of manipulator, its acceleration performance is degraded. In the region that the joint angle of the arm approaches to the desired angle, *a*~*b*, *c*~*d* in Fig. 10(a), the current is not applied not to interfere the movement of the arm, since the high response speed is required. In the region the arm passes the desired angle, i.e. the diagonally shaded areas of *b*~*c*, *d*~*e* in Fig. 10(a), a current is applied to improve the damping performance to converge to the desired angle quickly. To determine whether the magnetic field should be applied or not, the phase plane shown in Fig. 10(b) is used. The horizontal axis in the phase plane corresponds to joint angle deviation e between the desired angle θ_r and the joint angle θ, and the vertical axis corresponds to the derivation of the deviation $\dot{e} = \dfrac{de}{dt} = -\dot{\theta}$. Each point *a*~*e* on the phase plane corresponds to each point *a*~*e* in Fig. 10(a). Here, the region with the application of current is controlled by h[s^{-1}], the gradient of the line shown in Fig. 10(b). The region under the application of the damping torque expands as $|h|$ decrease.

The effectiveness of the proposed controller will be demonstrated through experiments with various external inertia loads.

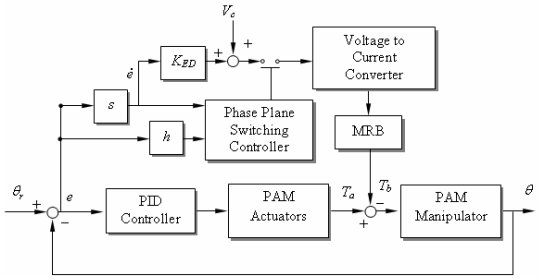

Fig. 9 Block diagram of control system

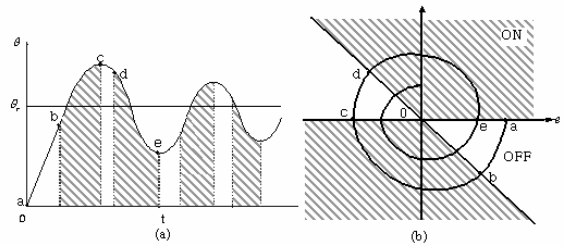

Fig.10 Concept of PPSC

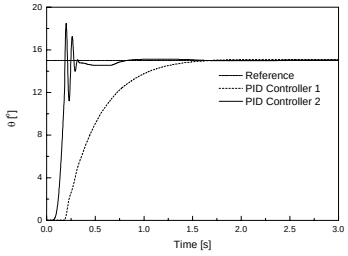

Fig. 11 Comparison between PID controller 1 and PID controller 2

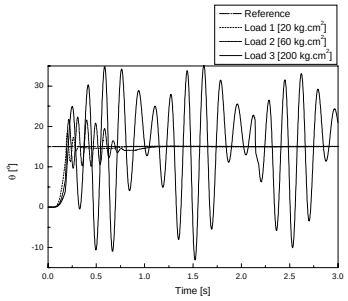

Fig. 12 Experimental results of PID controller 2 with various loads

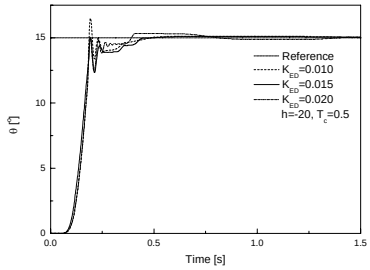

Fig. 13 Experimental results of proposed controller with various parameter of K_{ED}

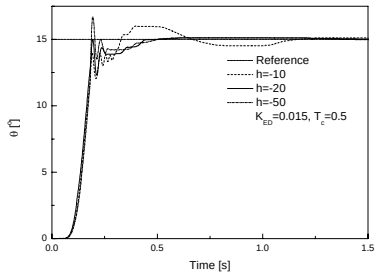

Fig. 14 Experimental results of proposed controller with various parameter of h

4. EXPERIMENT RESULTS

Experiments were carried out with 3 cases of external inertia loads $\left(20, 60, 200\, kg \cdot cm^2\right)$ and the comparison between the conventional PID controller and the PPSC was presented.

Figure 11 shows the experimental results of the conventional PID controller where the minimum external inertia load $\left(20\ kg \cdot cm^2\right)$ was used with the following 2 control parameters $K_p = 200\times10^{-6}, K_i = 1\times10^{-6}, K_d = 70\times10^{-6}$(PID controller 1) and $K_p = 1000\times10^{-6}$, $K_i = 10\times10^{-6}$ $K_d = 130\times10^{-6}$ (PID controller 2). It is obvious that it is difficult to satisfy both the damping and response speed. The manipulator must be controlled slowly in order to have a good stability. On the contrast, the overshoot and oscillation are always included if one wants fast response. In addition, experimental results with respect to 3 cases of external inertia loads $\left(\text{Load}\,1: 20\ \text{kg}\cdot\text{cm}^2; 2: 60\ \text{kg}\cdot\text{cm}^2; 3: 200\ \text{kg}\cdot\text{cm}^2\right)$ and PID controller 2 were shown in Fig. 12. From these results, it was understood that the system response became more oscillatory according to the increase of the external inertia load and became unstable with ten times bigger external inertia load.

Next, the experiments were carried out in practical PAM manipulator and the control parameters of the proposed controller, which was mentioned in Eq. (6), were set to be $T_c = 0.4, h = -20$ with various K_{ED} ($K_{ED} = 0.010, K_{ED} = 0.015, K_{ED} = 0.020$) in experiment condition 1 and $K_{ED} = 0.015, T_c = 0.4$ with various h ($h = -10, h = -20, h = -50$) in experiment condition 2. These control parameters were obtained by trial-and-error through experiments. The experimental results with respect to the experimental condition 1 and 2 were shown in Fig.13 and 14, respectively. In Fig. 13 and 14, the control parameters of PPSC were set to be $K_{ED} = 0.015, T_c = 0.4\ and\ h = -20$. All experiments were carried out by this condition of phase plane from now on.

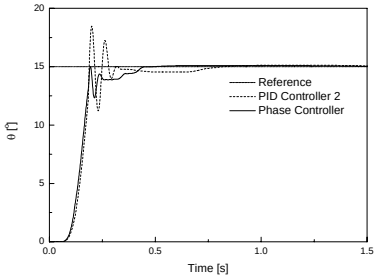

Fig. 15 Comparison between PID controller 2 and PPSC method (Load 1)

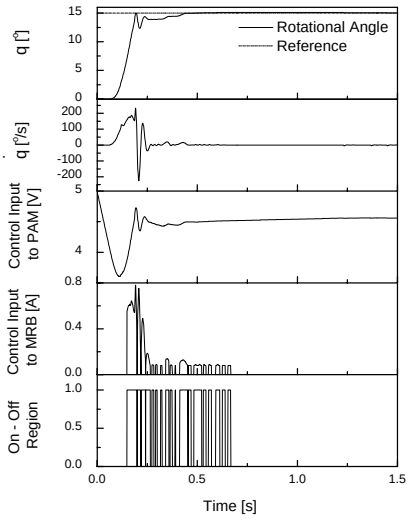

Fig. 16 Experimental results of PPSC(Load 1)

In Fig. 15, comparisons were made between the conventional PID controller 2 and the proposed controller with respect to load condition 1. In the experiments, the joint angle of PAM manipulator was in good agreement with that of reference and it was demonstrated

that the proposed algorithm was effective in this experimental condition. The region of damping and control input into MRB were shown in Fig. 16. The damping torque was not applied for fast response when the manipulator starts to move and the damping torque was generated by MRB to the rotational axis of PAM manipulator in order to reduce the overshoot and oscillation when the manipulator reaches the desired angle.

Next, experiments were executed to investigate the control performance with various external inertia loads. Figure 17 shows the comparison between the conventional PID controller 2 and the proposed controller with respect to the load condition 2. From the experimental results, it was found that a good control performance and strong robustness were obtained without respect to the variation of external inertia load by using PPSC method. In Fig. 18, the detail of the experiment of PPSC method with external inertia load condition 2 was shown. From this experimental result, the damping torque was applied and released very frequently according to the approach to the desired angle.

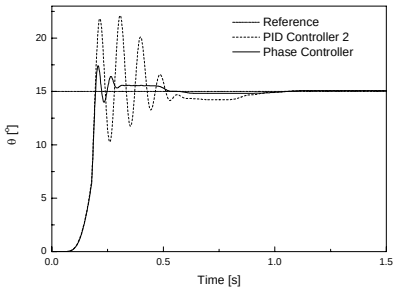

Fig. 17 Comparison between PID controller 2 and PPSC (Load 2)

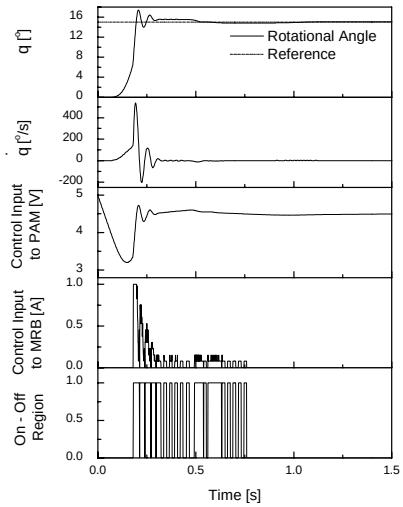

Fig. 18 Experimental results of PPSC (Load 2)

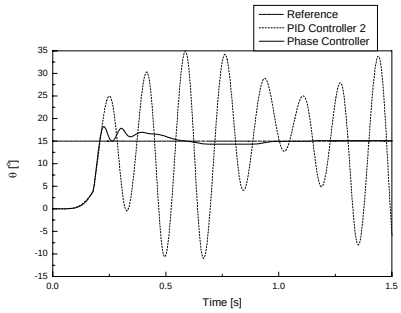

Fig. 19 Comparison between PID controller 2 and phase PPSC (Load 3)

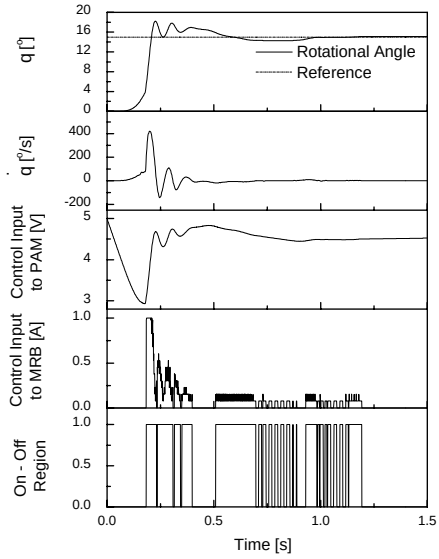

Fig. 20 Experimental results of PPSC (Load 3)

In Fig. 19, experiments were conducted to compare the system response of PID controller 2 and proposed PPSC under the external load condition 3. With up to ten times bigger external inertia load with respect to the minimum external inertia load, a good control performance was also obtained. Here, the steady state error was within $\pm 0.05\,[^0]$. Figure 20 shows the experimental results of PPSC method in detail with respect to the external inertia load condition 3. It was concluded that the proposed controller was very effective in the high gain control, fast response and robust stability with ten times changes of external inertia load.

However, there still remain some problems such as the difficulty of the selection of the optimal control parameters of proposed PPSC in order to get a good control performance of the PAM manipulator, especially with various external inertia loads.

There is no previous research to find optimal control parameters in case of PPSC method up to now. As future study, we are planning to design a new intelligent control algorithm using neural network with PPSC method, which utilizes the adaptive and learning capabilities of neural network in order to find the optimal control parameters with respect to various external inertia loads.

5. CONCLUSION

In this paper, a new PPSC method using the magneto-rheological brake was applied to the pneumatic artificial muscle manipulators in order to improve the control performance with various external inertia loads.

From the experimental results, the newly proposed controller was very effectively in high gain control with respect to the 1,000 [%] external inertia load variation. And the steady state error with respect to various loads was reduced within $\pm 0.05\,[^0]$. It was verified that the proposed control algorithm presented in this study had simple structure and had better dynamic property, strong robustness and it was suitable for the control of various plants, including linear and nonlinear process, compared to the conventional PID controller.

By using MRB as a variable damper, the damping torque was controlled by the applying magnetic field strength and the position control performance was improved without the decrease of response speed by separating the region, where the damper produces an damping torque by PPSC method.

The results show that the MRB is one of effective methods to develop a practically available human friendly robot by using the PAM manipulator.

REFERENCES

1. Zobel, P. B., Durante, F. and Raparelli, T., "The experience of the University of L'Aquila on the PAM actuators for a 2 DOF manipulator for function recovery therapy," Seminar on Biomechanics, (1999).
2. Klute, G. K., Czerniecki, J., and Hannaford, B. , "McKibben Artificial Muscles: Actuators with Biomechanical Intelligence," Proc., IEEE/ASME Int., Conf., Advanced Intelligent Mechatronics (1999), pp. 221~226.
3. Koeneman, E. J., Schultz, R. S., Wolf, S. L., Herring, D. E. and Koeneman J. B., "A pneumatic muscle hand therapy device," Proc., IEEEInt., Conf.(2004), pp. 2711-2713.
4. Hesselroth, T., Sarkar, K., Patrick van der Smagt, P., and Schulten, K., "Neural network control of a pneumatic robot arm," IEEE Trans Syst., Man., Cybernetics., Vol. 24 (1994), No 1, pp. 28~38.
5. Patrick van der Smagt, P., Groen, F., and Schulten, K., "Analysis and control of a Rubbertuator arm," Biol. Cybernet., Vol. 75 (1996), pp. 433~440.
6. Caldwell, D. G., Medrano-Cerda, G. A., Goodwin, M. j., "Characteristics and adaptive control of pneumatic muscle actuators for a robotic elbow," in Proc., IEEE Int., Conf. Robotics and Automation, Vol.4 (1995), pp. 3558~3563.
7. Bowler, C. J., Caldwell, D. G., and Medrano-Cerda, G. A., " Pneumatic muscle actuators; Musculature for an anthropomorphic robot arm," in Proc. IEE Colloqium on Actuator Technology Current Practice and New Developments, London (1996), pp. 8/1~8/5.
8. Tondu, B., and Lopex, P., "Modeling and control of Mckbben artificial muscle robot actuators." IEEE Contr., Syst., Mag., Vol. 20 (2000), No. 1, pp. 15~38.
9. Chan, S.W., Lilly, J.H., Repperger, D.W., Berlin, J.E., "Fuzzy PD+I learning control for a pneumatic muscle," in IEEE Int., Conf., Fuzzy Systems, Vol. 1 (2003), pp. 278~283.
10. Cai, D., Yamaura, H., "A VSS control method for a manipulator driven by an McKibben artificial muscle actuator," Electron, Commun, Japan, Vol. 80, No. 3 (1997), pp. 55~63.
11. Iskarous, M., Kawamura, K., "Intelligent control using a neuro-fuzzy network," in Proc., IEEE/RSI Int., Conf., Intelligent Robots and Systems, Vol. 3 (1995), pp. 350~355.
12. Folgheraiter, M., Gini, G., Perkowski, M., and Pivtoraiko, M., "Adaptive Reflex Control for an Artificial Hand," in Proc., , Symposium on Robot Control, (2003).
13. Noritsugu, T., Tanaka, T., "Application of rubber artificial muscle manipulator as a rehabilitation robot," in IEEE/ASME Trans., Mechatronics, Vol. 2 (1997), pp. 259~267.